FEATURE ARTICLE

ChemComm
www.rsc.org/chemcomm

# Shape-persistent arylene ethynylene macrocycles: syntheses and supramolecular chemistry

**Dahui Zhao and Jeffrey S. Moore***
*Departments of Chemistry and Materials Science & Engineering, University of Illinois, Urbana, IL 61801, USA. E-mail: moore@scs.uiuc.edu*

*Received (in Cambridge, UK) 30th July 2002, Accepted 14th October 2002*
*First published as an Advance Article on the web 15th November 2002*

**This article describes recent developments in the synthesis of macrocycles having rigid, monocyclic skeletons composed of arylene and ethynylene units and the studies on their self-assembling behavior.**

## Introduction

Macrocycles having rigid, non-collapsible, unsaturated hydrocarbon backbones have attracted great interest in the past few years, due to their novel properties and potential applications.[1–6] Among the macrocycles that have these characteristics, one particular group has distinguished itself by demonstrating tremendous synthetic versatility and the ability to spontaneously organize into ordered assemblies. These macrocycles consist of a shape-persistent scaffold comprised of arylene and ethynylene units in a planar or nearly planar conformation, with a minimum of ring strain and a large diameter to thickness ratio (typically, nanoscale in diameter and *ca.* 3.5 Å thick). Often they possess an internal void volume because of their toroidal shape. The cyclic backbone of these macrocycles is typically modified with peripheral side chains containing various functionalities, which gives rise to their unique and interesting behavior. A diversity of supramolecular assemblies, including three-dimensional nano-structures, discotic liquid crystals, extended tubular channels, guest–host complexes and porous organic solids, may be realized by these shape-persistent arylene–ethynylene macrocycle (AEM) building blocks.

Motivated by the novel properties and potential applications of these self-assembled entities, intense efforts have been made to explore highly efficient methodologies for preparing such macrocycles with varied structures. Studies into supramolecular organizations of these macrocycles have provided a better understanding of the non-covalent driving force responsible for their self-association. Since a vast amount of work has been carried out in this area and there have been elegant previous reviews addressing related topics,[1–6] this article will be devoted to the most recently developed synthetic methods for constructing AEMs, and to the studies aimed at understanding and/or controlling their association in solution, in mesophases, at the air-water interface and in the solid state.

*Dahui Zhao was born in China in 1974. She received her B.S. in Chemistry in 1997 from Beijing University. Currently she is a PhD student with Professor Moore, working on reversible syntheses of imine-containing m-phenylene ethynylene polymers and macrocycles.*

*Jeffrey Moore was born outside of Joliet, IL in 1962. After receiving his B.S. in chemistry from the University of Illinois (1984), he completed his Ph.D. in Materials Science and Engineering, also at the University of Illinois, with Samuel Stupp (1989). He then went to Caltech as a NSF postdoctoral fellow to study with Robert Grubbs. In 1990 he joined the chemistry faculty at the University of Michigan in Ann Arbor, but returned to the University of Illinois in 1993 where he is currently a Professor of Chemistry and Materials Science and Engineering. His current research focuses on molecular self-assembly and self-organization, structure-controlled macromolecules and foldamers, stimuli-responsive materials, and materials and methods for nano- and mesoscale devices.*

## Syntheses of arylene–ethynylene macrocycles

In considering general and useful building blocks for supramolecular constructions, size and shape of the molecules are two of the most important factors. In this context AEMs offer special opportunities. By engineering large, information-rich molecular surface in AEMs, it will become possible to use collections of weak, non-specific van der Waals and hydrophobic forces in a more controlled fashion to assemble chemical species with well-defined, structural and functional complexity. The characteristics of the resulting supramolecular entities are dictated by the physical and chemical features of each composing macrocycle. In this light, the importance of synthesizing macrocycles with pre-designed structures becomes eminent.

### Geometrical shape design

Phenylene and ethynylene monomers provide a versatile and convenient approach toward modular construction of cyclic structures. Any framework of varied size with a geometric shape consistent with a trigonal lattice is accessible by using combinations of a small set of building blocks: *ortho*-, *meta*- and *para*-phenylenes (having bond angles of 60, 120 or 180°, respectively).[6] The ethynylene unit spaces apart these aromatic rings far enough such that adjacent units do not sterically interact, as in biphenyl. Shape-persistency of the overall framework follows from the rigidity of each composing fragment. Fig. 1 gives a few examples of such cyclic structures of different shape and size.

As will be shown later, the shape of AEMs plays a critical role in determining the packing motif when these molecules self-assemble into supramolecular structures. Their geometrically well-defined (shape-persistent) skeletons are effective at positioning and orienting steric and electronic features that dictate intermolecular interactions. Therefore, the shape, together with functionalization, of these structures can be viewed as the information that makes up the complete set of instructions for all the subsequent supramolecular chemistry.[1,6]

DOI: 10.1039/b207442g

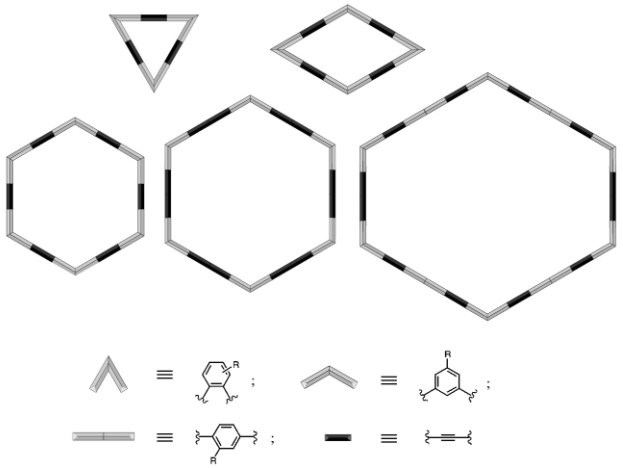

**Fig. 1** Schematic representations of phenylene–ethynylene macrocycles and the building blocks from which they are constructed.

### Backbone construction and cyclization strategies

In joining different constituent fragments into a macrocycle, the carbon–carbon bond formation between the arylene and ethynylene units represents one of the major tasks. With the rapid developments in transition metal catalyzed synthetic methodologies, coupling reactions between $sp^2/sp$ and $sp/sp^2$ carbons have become routine in organic syntheses,[7] and the preparations of various AEMs have definitely benefited from the progress in this area of synthetic methodology. A variety of reactions have been used to facilitate carbon–carbon bond formation between arylene and ethynylene units in AEM syntheses (Fig. 2). For example, palladium-catalyzed Sonogashira–Hagihara cross coupling[7,8] has prevailed in joining aryl halide and terminal alkyne to generate ethynyl–aryl bonds.[1,9–12] Hay,[13] Eglinton-Glaser homocoupling[14] and palladium-catalyzed hetero-coupling[15] between terminal alkynes are most commonly used in furnishing butadiyne units;[16–26] Suzuki cross-coupling between aryl halides and aryl boronic acids, or esters, has been adopted in synthesizing aryl–aryl moieties.[27–29]

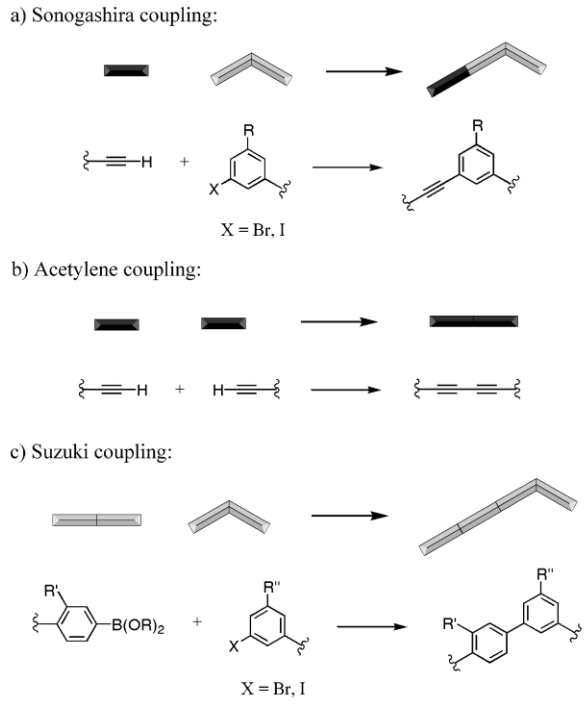


**Fig. 2** Representative carbon–carbon bond forming reactions used in backbone constructions of phenylene–ethynylene macrocycles.

Strategies that have been used in these macrocycle syntheses can be categorized into three major types (Fig. 3): (i) one-step oligomerization/cyclization; (ii) intramolecular ring-closure of bisfunctionalized oligomers; (iii) intermolecular coupling between two or more ring fragments followed by unimolecular cyclization in one pot—a hybrid of the first two approaches.

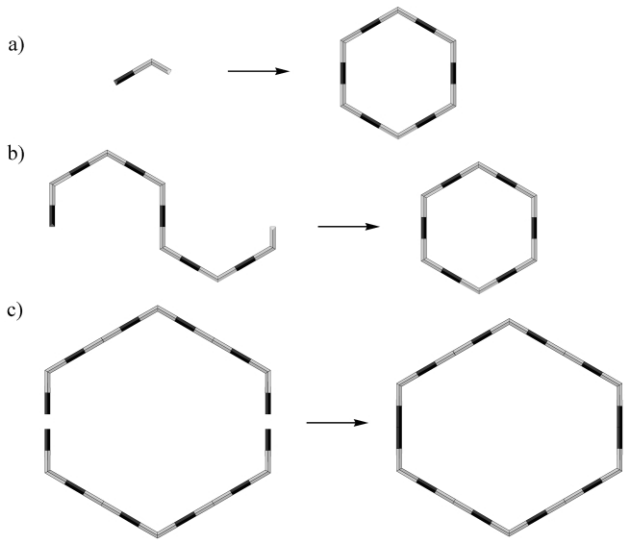


**Fig. 3** Representative schematic of cyclization strategies: (a) one-step oligomerization/cyclization method; (b) intramolecular cyclization; (c) bimolecular coupling/unimolecular cyclization.

The first synthesis of a hexakis(*m*-phenylene–ethynylene) macrocycle **1** was accomplished by Staab and Neunhoeffer as early as 1974, through six-fold Stephens–Castro coupling of copper *m*-iodophenyl acetylide (Scheme 1(a)).[30] This method presents an example of the one-step oligomerization/cyclization strategy. It starts from precursors containing a single repeating unit and the cyclization proceeds in competition with chain elongation into oligomers and polymers in one pot. More recently, the same strategy was applied by Bunz and coworkers in preparing a similar AEM, **2**.[31] Starting from a dipropynyl substituted benzene derivative, this macrocycle was synthesized *via* a novel method for generating carbon–carbon triple bonds—alkyne metathesis (Scheme 1(b)).[32] Although the scope and the functional group compatibility of alkyne metathesis is still awaiting further development, this reaction has offered a feasible alternative for producing linear and cyclic poly(arylene–ethynylene) chains.[33]

The advantage of this one-step procedure is evident; the starting materials are readily accessible and the target molecule is generated in a single step. However, the yields of these reactions were inevitably low (4.6 and 6% in the case of Staab and Bunz, respectively), because the desired cyclic structure must compete against a broad, statistical distribution of products that includes all linear/cyclic oligomers/polymers of different chain length. Moreover, macrocyclization is a unimolecular process that is intrinsically disfavored by entropy (due to the loss of conformational freedom), but the reactions must be run under conditions that favor bimolecular couplings by which means the cyclization precursor is afforded. Additionally, the generation of large quantities of polydisperse byproducts with similar structures has made the separation and purification of the target molecule extraordinarily difficult.

Obviously, this crucial drawback made the procedure impractical for producing large quantities of materials. Consequently, after the initial work by Staab, further investigations on such macrocycles were nonexistent for almost two decades

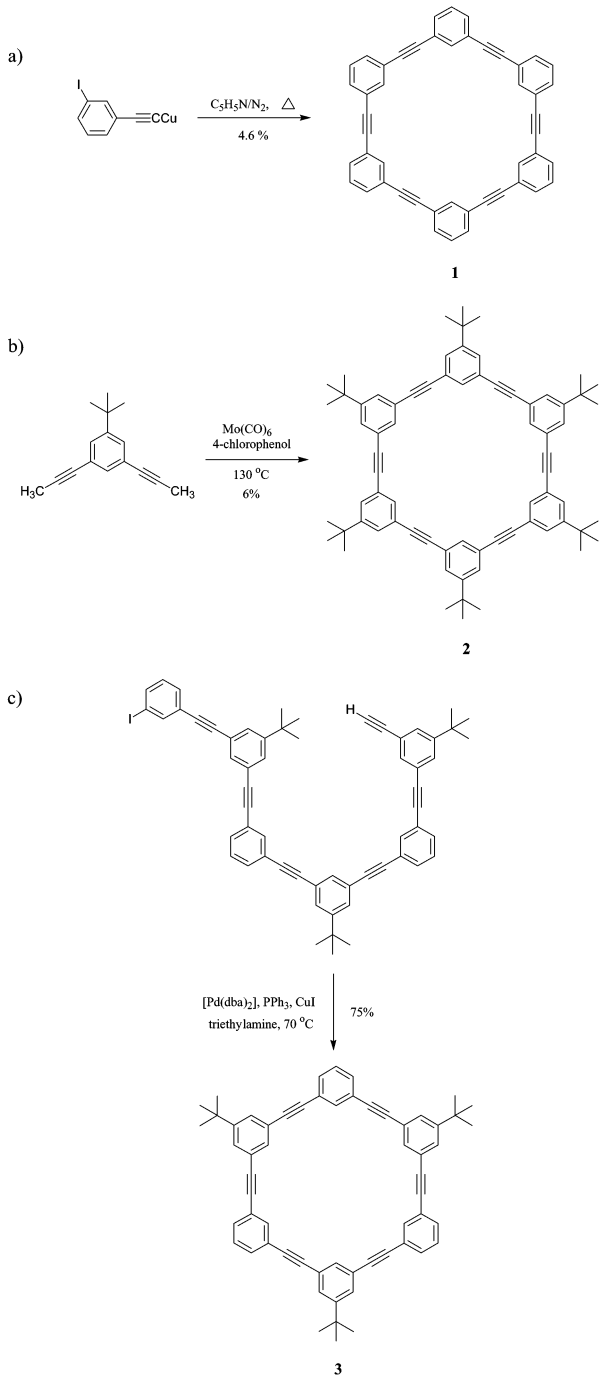


**Scheme 1** Examples of one-step oligomerization/cyclization ((a) and (b))[30,31] and intramolecular cyclization (c).[9]

when Moore and coworkers employed modern synthetic methods and developed a versatile and efficient route to synthesize AEMs.[9,10]

Motivated by precise structural control, Moore and Zhang performed the syntheses of a series of AEMs (such as **3** in Scheme 1(c)).[9] Using Pd–Cu catalyzed cross-coupling and a pair of efficient, orthogonal protecting groups, a series of α-iodo-ω-ethynyl functionalized *m*-phenylene–ethynylene oligomers having well-defined homo- and hetero-sequences were synthesized (Scheme 2).[10] Upon subsequently conducting an intramolecular ring-closing Sonogashira reaction under pseudo-high dilution conditions (*i.e.*, slow addition of oligomers to a catalyst solution) desired macrocycles were generated in moderately high yields (*ca.* 60–80%).[10] The remarkably improved yield of macrocycles was attributed to the pre-organization of the cyclization precursors. Moreover, highly dilute conditions can be applied since intermolecular reactions are no longer required, and unimolecular cyclization consequently becomes kinetically more favorable than bimolecular coupling. In addition to the yield improvement, several consequences of pre-organization of oligomeric precursors made this stepwise procedure superior to the one-step method. First, the convergent, stepwise syntheses of phenylene–ethynylene oligomers allowed for absolute control over the size and functional group placement of the subsequently formed macrocycles. Various side-chain functionalities can thus be precisely positioned according to design requirements. Second, macrocycles with different geometrical shapes could readily be achieved by controlled incorporation of *ortho*-, *meta*- and *para*-phenylene–ethynylene fragments into the oligomer sequence. Importantly, this methodology could be adapted to a wide variety of coupling reactions in the cyclization of AEMs having diverse backbone structures.[11,22–26]

Although the intramolecular ring-closure provided the greatest versatility for structural control, there is a drawback to this methodology: preparation of the precursor oligomers is time-consuming since iterative protecting, deprotecting and coupling steps are involved. An alternative strategy that combined the advantages and circumvented the shortcomings of the above two extremes was then investigated by a number of groups.[17,22,27,34] It was discovered that, given appropriate chain length and suitable terminal functionality, a pair of oligomers can undergo an intermolecular coupling followed by an intramolecular cyclization in one pot, furnishing macrocycles in satisfactory yields (Scheme 3). Although this method usually gives lower yields than the intramolecular macrocyclization, fewer synthetic steps to the precursors are required, thereby enhancing the overall yield and making this procedure more time-efficient. However, further breaking down the cyclization precursors into three or more pieces led to less desirable cyclization yields.[18] Significantly, this bimolecular coupling/unimolecular cyclization strategy has proven applicable to a variety of coupling reactions, including Sonogashira,[35–38] oxidative Eglinton–Glaser,[19,21,25,26] Suzuki couplings[27–29] and imine condensation[34] and metathesis,[39] generally furnishing satisfactory yields.

Another noteworthy characteristic of AEM syntheses is the utility of the differential reactivities of iodo- and bromo-substituted arenes toward Sonogashira coupling. Selective deprotection of triisopropylsilyl- and trimethylsilyl-ethynyl groups has also been frequently used with great success. Both of these protocols have helped to substantially reduce the number of protecting–deprotecting steps.[17,22,36]

## Solid-phase synthesis

Solid-phase synthesis has become a widely practiced method in organic chemistry, due to its distinct advantage of convenient procedure, ease of purification and high efficiency. This powerful synthetic tool was used to prepare sequence-specific phenylene–ethynylene oligomers as AEM precursors as early as 1994.[40]

An especially appealing characteristic of solid-phase synthesis to macrocycle researchers is its potential of spatially separating functional groups. Since the reactive species is covalently immobilized onto the polymeric support, intermolecular reactions were expected to be greatly minimized and intramolecular ring closure should thus dominate (Fig. 4(a)). Rothe and coworkers first tested the feasibility of this premise by cyclizing polymer supported amino acid oligomers.[41] More recently, Tour and coworkers applied this strategy to the macrocyclization of phenylene–ethynylene oligomers.[42] Unfortunately, both of these studies reached the conclusion that the solvated polymer resins were not rigid enough to provide

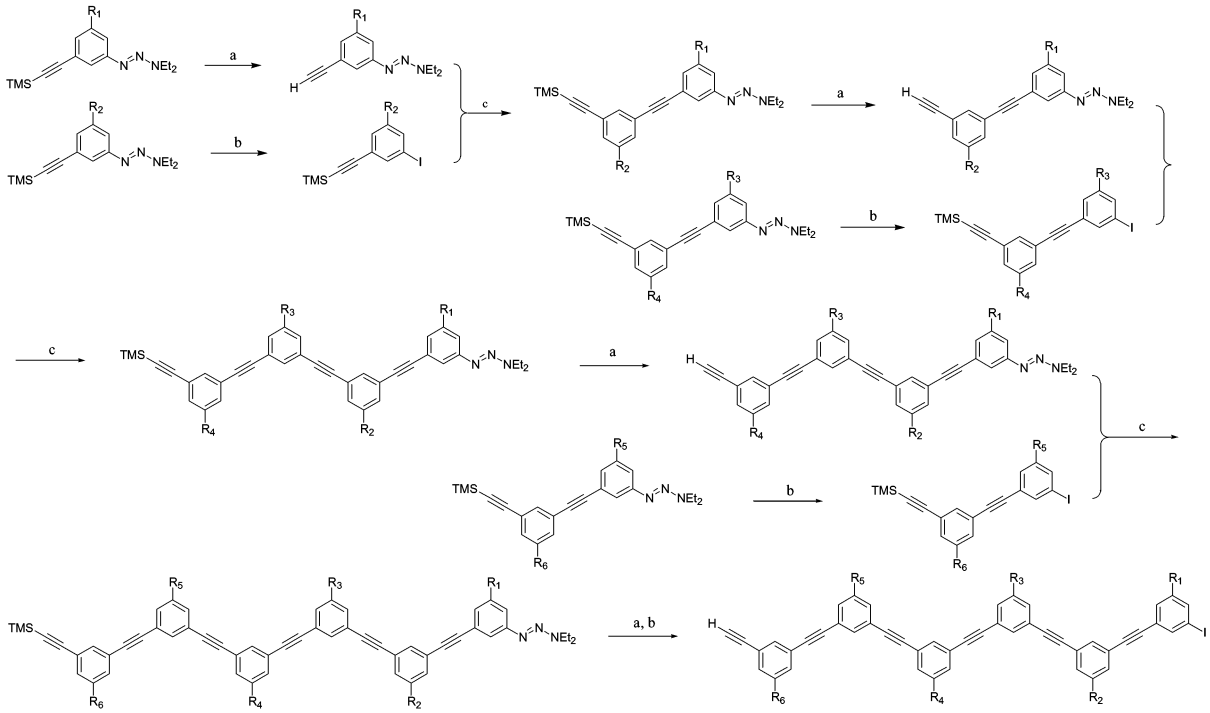

**Scheme 2** Iterative synthetic route to a representative α-iodo-ω-ethynyl *m*-phenylethynylene oligomer.[10] *Reagents and conditions*: (a) MeOH, $CH_2Cl_2$, $K_2CO_3$ or tetrabutylammonium fluoride, THF, rt; (b) $CH_3I$, 110 °C; (c) $Pd(dba)_2$, CuI, $PPh_3$, triethylamine, 80 °C.

complete site isolation and intersite reactions were observed (Fig. 4(b)). Although the polymer supported cyclization has not been completely successful, its potential should be further explored.

### Templated cyclization

Although pre-formation of the oligomers and the rigidity of the phenylene–ethynylene backbone greatly helped improve the macrocycle yield, the efficiency of the cyclization was still only modest in some cases. Additional measures have been taken to further optimize the macrocyclization step, such as conducting the reaction under high-dilution conditions. However, this practice only partially prevented oligomerization and demanded large amounts of solvent.

In order to more effectively increase the ratio of cyclic to linear products, a template methodology was explored, first by Sanders and Anderson in the synthesis of porphyrin-containing macrocycles.[43] In their design, oxidative cyclization was carried out in the presence of a template that was able to simultaneously bind to a certain number of reactants through metal–ligand coordination interactions. Different sized macrocycles, depending on the number of the ligands incorporated in the template, were obtained in much higher yield than in the absence of the template. Later on, a covalently attached template was introduced by Höger *et al.* for synthesizing AEMs (Scheme 4).[4,18,20] Nearly quantitative macrocyclization yield was obtained with the covalent template.

The basic concept behind the templating approach involves the pre-organization of the reaction precursors such that the local reactant concentration is considerably increased, thereby greatly facilitating cyclization. In these templated reactions, the size of the macrocycle may vary with the number of fragments bound to the template. Accordingly, the size can be controlled through template design.[43] Covalently-attached templates usually require the introduction of specific functional groups into the substrates (cyclization precursors in these cases), and extra synthetic steps may be needed for attachment and cleavage. However, the extraordinary yield, even in coupling more than two fragments in one pot,[18] has made this methodology quite appealing. Non-covalent templates may be superior to covalent ones in terms of the traceless and reversible nature.

### Aggregation-driven reversible macrocyclization

Due to significant developments in the field of dynamic combinatorial chemistry, there has been a resurgence in exploiting equilibrium controlled syntheses aimed at accessing thermodynamically stable products.[44] Under reversible conditions, all the reaction products are dynamically interconvertible and the product distribution is dictated by thermodynamic stabilities. Dynamic synthesis therefore offers an alternative pathway to AEMs under conditions that render macrocycles the thermodynamically most stable products.

The synthesis of an AEM by reversibly forming a pair of covalent bonds in the backbone has recently been reported.[34] Significantly, a nearly quantitative conversion into macrocycle **4** was yielded by refluxing oligomers **5** and **6** in methanol at relatively high concentration (Scheme 5). It was surprising that the reversible imine condensation could proceed to almost completion, exclusively generating the macrocycle, even though no efforts were made to remove the condensation byproduct water out of the system. In order to further elucidate the driving force for the high conversion to the macrocycle, a different coupling reaction—imine metathesis, was employed to prepare the same macrocycle.[39] Interestingly, the imine metathesis mediated cyclization between **7** and **8** exhibited a strong solvent dependence: in chloroform, the yield of the desired macrocycle **4** was much lower than in acetonitrile, wherein nearly quantitative conversion was obtained. These observations were explained as follows: during its synthesis, the macrocycle was stabilized by intermolecular aromatic stacking interactions bringing about aggregation in polar solvents such as acetonitrile and methanol (*vide infra*).[34,45] Hence, the assemblies of stacked macrocycles became the thermodynamically most favorable product; the comprising unit **4** was thus predominantly formed.[34,39] These results demonstrated that

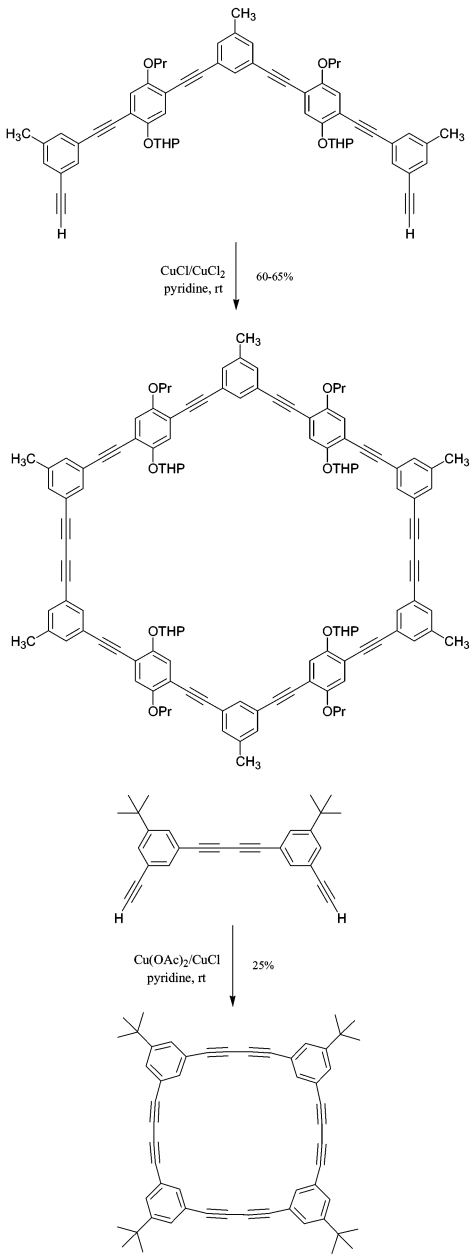


**Scheme 3** Examples of bimolecular coupling/unimolecular cyclization.[17,22]

dynamic covalent synthesis offers a highly efficient route to AEMs provided that conditions are appropriate.

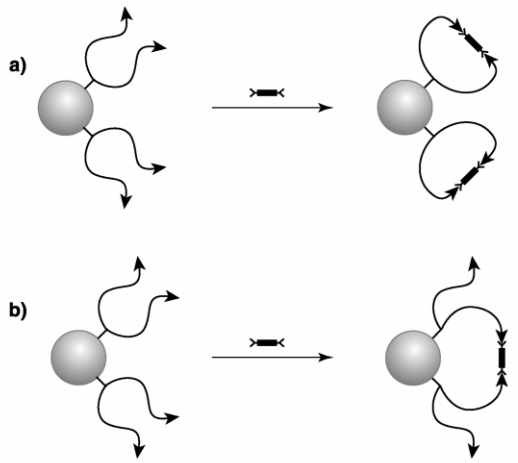


**Fig. 4** Schematic representation of solid-phase synthesis: (a) site isolated macrocyclization; (b) inter-site reaction.

### Side chain attachment

As mentioned earlier, most of the AEMs are decorated with various pendant functional groups. Two different approaches have generally been adopted for attaching side chains onto the backbone: first, joining monomer units bearing the desired side chains into a macrocycle; second, conducting functional group transformation upon cyclization.[10,21,46] Although both methods have proven viable in synthesizing AEMs, with properly developed chemistry the latter may offer more synthetic economy by allowing more convenient structural variation through pendant group modification.

## Supramolecular organizations of arylene–ethynylene macrocycles

Having a rigid, non-collapsible backbone with a large aromatic surface, AEMs tend to stack face-to-face in solution and the condensed states, maximizing their area of contact and thus van der Waals and π–π stacking interactions.[47,48] In solution, the strength of aromatic stacking among AEMs has been found to strongly depend on the solvent, presumably due to the solvophobic nature of the association.[11,49]

The fact that aromatic stacking and solvophobic effects are weak in strength is one of the reasons why these interactions have been difficult to study experimentally and understand theoretically. In an AEM, multiple aromatic units are joined into a cyclic scaffold. Due to the rigidity of the resulting structure, the entropy loss (translational and rotational) during AEM dimerization is not much greater than that of stacking two properly oriented small molecules containing a single aromatic

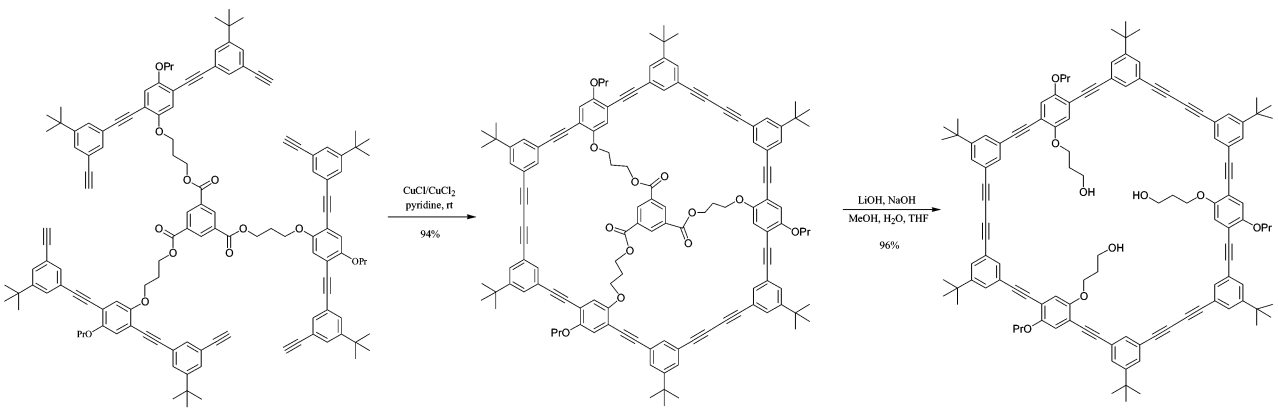


**Scheme 4** Representative template directed synthesis of a phenylene–ethynylene macrocycle.[18]

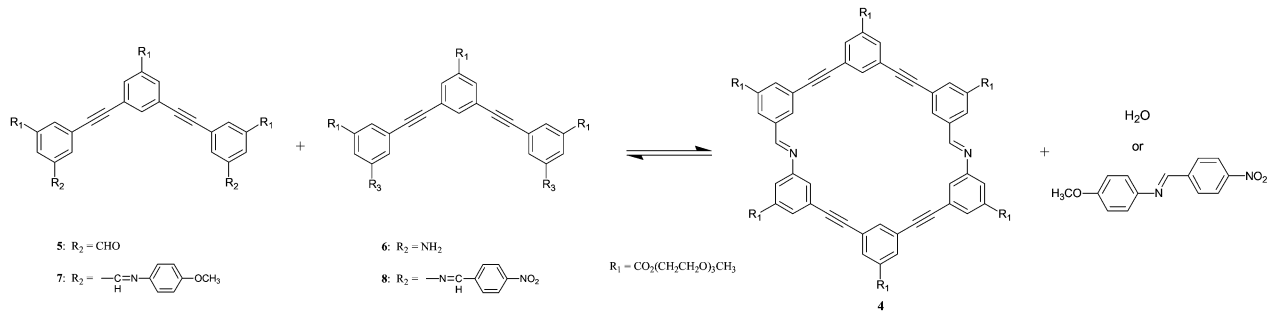


**Scheme 5** Thermodynamically controlled macrocyclization *via* reversible imine condensation[34] or metathesis.[39]

unit. However, the much larger surface area of the macrocycle provides multiplied driving force for the association between AEMs. Thus, the weak, pairwise interactions are cooperatively amplified when the macrocycles associate with one another. This unique feature of AEMs makes them ideal models for studying the aromatic and solvophobic interactions.

Two different stacking motifs, edge-to-face and offset face-to-face, are exhibited by interacting aromatic molecules. The latter has been predominantly observed with AEMs. This is not surprising considering that by stacking face-to-face the macrocycles benefit from the maximum number of interacting units, while the side chains that are normally present in AEMs to improve solubility also disfavor edge-to-face association.

## Aromatic stacking interactions

As solvophobically favored aromatic stacking is a crucial driving force for the aggregation of AEMs, a better understanding and control of this interaction would be useful in predicting the self-association behavior and designing AEMs to achieve self-assembled structures with desired properties.

Aromatic stacking[47,48] has long been recognized as playing an important role in diverse areas, such as protein and DNA structures, supramolecular chemistry, molecular recognition, stereocontrol of organic reactions, and solid-state packing of aromatic molecules. Quantitative analysis of this interaction is complicated by the involvement of several factors including van der Waals, solvophobic and electrostatic effects. However, some qualitative conclusions can be drawn from the vast amount of research dedicated to this field. First, van der Waals and solvophobic interactions make significant contributions to aromatic stacking related associations. Studies have shown that both the surface area[50] and the nature of the solvent strongly affect the strength of π-stacking.[11,49,51] Second, electrostatic interactions are also important, as the aromatic association has been shown to be dramatically influenced by the electronic characteristics of the substituents attached to the aromatic groups.[11,52–55] These observations can be explained by an electrostatic model introduced by Hunter and Sanders, in which the electrostatic driving force of aromatic interactions is proposed to come from an attraction between the positively charged σ-framework and the negatively charged electron cloud of the interacting units.[48]

## Association in solution

Chemical shift changes in nuclear magnetic resonance (NMR) spectroscopy have been well documented as a signature of aromatic stacking.[56] When two or more aromatic units come into close vicinity of each other, the nuclei of one molecule are affected by the ring-current magnetic anisotropy of the other, resulting in resonance shifting,[57] typically upfield due to the offset geometric arrangement of the interacting units. Since the NMR data are usually accurate, readily available and require a relatively small amount of sample, this technique has widely been adopted to study aromatic associations in solution.

Another commonly used technique in the investigations of AEM aggregation in solution is vapor pressure osmometry (VPO). Osmotic measurement is based on colligative effects and provides a measure of the number average molecular weight. The VPO technique complements NMR in that it is able to distinguish systems in which monomer–dimerization equilibrium dominates from those wherein higher aggregates form. This piece of information is important because, as will be discussed next, it helps to determine which type of model should be applied in determining association constant from experimental data. Since NMR spectroscopy measures short-range effects of aromatic stacking interaction while VPO offers a macroscopic view of average aggregation degree, it is not surprising that discrepancies may occur when comparing independent data from the two techniques.[26]

In order to obtain quantitative information on the association strength, experimental data from NMR or VPO are usually applied to theoretical models and interpreted into association constants. A variety of mathematical models have been proposed to explain intermolecular associations and a number of them have been employed in analyzing AEM aggregation in solution.[56,58-60] In these models, the association processes are described in the form of a series of equilibrium equations. Since the thermodynamic equilibrium state is of major concern, rather than the kinetically most favored pathway or the mechanism of aggregate formation, the selection of expressions does not affect the fitting result, as long as all the possible complexes and the corresponding equilibrium constants are appropriately included. Eqn. (1) is the most commonly used set of expressions, in which the association is described as successive addition of a monomer unit onto another monomer or an existing aggregate. The observed average degree of association from VPO experiments can be fitted by adjusting variables in the model, such as the association constants. The best-fit association constants can thus be determined. Additional parameters are required in analyzing concentration dependent NMR chemical shift data, *e.g.*, the chemical shifts of the monomer, the terminal, and the internal units of a stack when the nearest-neighbor effect is taken into account.[56] Including longer range effects of neighboring interactions requires more chemical shift related parameters.[56]

$$\begin{aligned} A + A &\overset{K_2}{\rightleftharpoons} A_2 \\ A_2 + A &\overset{K_3}{\rightleftharpoons} A_3 \\ A_3 + A &\overset{K_4}{\rightleftharpoons} A_4 \\ &\vdots \\ A_{i-1} + A &\overset{K_i}{\rightleftharpoons} A_i \\ &\vdots \end{aligned} \qquad (1)$$

The simplest and most commonly used model in studying AEM aggregation is the monomer–dimer model.[58] In this model, it is assumed that monomer–dimer equilibrium is the only association process and no aggregates higher than dimer are formed (*i.e.*, $K_{n>2} = 0$). Such a model can be used in systems where dimerization is the predominant process and the association into higher aggregates is negligible. This takes place with many AEMs in medium polar, chlorohydrocarbon solvents such as chloroform.[21,26,38,54,55] When higher aggregates form,[11,26] different models that accommodate higher order associations, either finite[59] (or capped, *i.e.*, $K_{n>i} = 0$) or infinite ($K_{n\rightarrow\infty} \neq 0$) mode,[56,60] may be adopted. Another aspect in which the models may vary is the interdependence of the association constants. For most AEMs that do not possess charge or experience severe steric interaction during aggregation, the free energy for each association step described in eqn. (1) should not vary substantially, and therefore an isodesmic model in which all the association constants are identical is plausible.[11,26] When the isodesmic model fails to give a satisfactory fitting result, varied $K$ models must be employed.[26,34] The dimerization constant, $K_2$, may be allowed to differ from the rest of the series, as it corresponds to association between two monomeric species, while a monomer and an aggregate are involved with the rest. The equilibrium constants of these subsequent additions can either maintain a constant value, increase or attenuate as the stack grows.[56,60]

A good agreement between the calculation based on the model and the experimental data is a necessary but not sufficient requirement to validate a model. Given enough independently adjustable parameters, any model is able to give reasonably good fitting. Therefore, physical explanation, in addition to mathematical fitting, is necessary to justify the association behavior described by a certain model.

In 1992, Zhang and Moore first reported the concentration dependent chemical shift of macrocycle **9** in a chloroform solution.[54] This observation suggested that the macrocycle was aggregating at higher concentration, presumably due to the intermolecular aromatic stacking interactions. Subsequently, the dimerization constants of a series of *m*-phenylene–ethynylene macrocycles with different functional side groups were determined and analyzed systematically.[54,55]

The self-association abilities of these macrocycles were found to vary with the structures of both the backbone and the side chains (Table 1). It was found that among all the macrocycles studied, those having exo-annular linear alkyl side chains linked to the backbone through benzoic ester groups (**9**–**12**) favorably formed aggregates within the investigated concentration range. As long as the alkyl group remained unbranched, the length of the side chains had a negligible effect on the association strength. However, the association propensity was significantly diminished by simply reversing the direction of the ester linkage. No concentration dependent chemical shifting was exhibited by **13**, a constitutional isomer of **9**. Similarly, neither benzyl ether or phenyl ether side chain linkages (**14**–**15**) promoted self-association behavior. These results supported the notion that aromatic association was sensitive to the electrostatic property of the aromatic units and was favored by electron-withdrawing substituents.[48]

Mixed information was obtained on whether a donor–acceptor effect was contributing to the stacking. Macrocycles **16** and **17**, having binary substituents, exhibited overall decreased association constants at room temperature compared to **9**. The thermodynamic parameters derived from variable temperature NMR data suggested that there was a favorable enthalpic gain during the aggregations of **16** or **17** (likely from donor–acceptor interactions), and that the decreased association constants at room temperature was a result of an unfavorable entropy change (possibly due to an highly ordered stacking motif). On the contrary, there was evidence showing that **9** formed homo- rather than heteroaggregates in the presence of **14** or **15**.[54] These results indicated that the strength of a donor–acceptor interaction was at most modest and easily compensated by the interactions between electron-deficient groups, as predicted by Hunter and Sanders' model.[48]

Steric hindrance was shown to be a factor that inhibits π-stacking, as evidenced by the absence of intermolecular aggregation in **18** which had bulky *tert*-butyl ester groups as side chains. Additionally, macrocycle **19** (an isomer of **16**), having three *endo*-annular side chains, did not exhibit concentration dependent chemical shifts.[54] Presumably, in this case, steric repulsions among the *endo*-side chains blocked association, since the electronic property of the aromatic framework of **16** and **19** is not substantially different.

The tendency of AEMs to undergo self-association was also found to be sensitive to ring size. Both **20** and **21** furnished much lower association constants than **9**. The diminished aggregation stability of **20** could not be completely explained by a simple proportional reduction in free energy due to the loss of one phenylene unit, since a much larger decrease in association constant was observed. The attenuated association of **21** was attributed to its non-planar geometry and conformational flexibility as revealed by a molecular mechanics study.[55]

The association constants of the above macrocycles were determined by applying the $^1$H NMR data to the monomer–dimer model. The aggregate size and association constants were independently verified by VPO studies. It was confirmed that aggregates beyond the dimer were not significantly formed in chloroform. Additionally, in these macrocycles, the calculated association constants based on independent NMR and VPO data were in good agreement.[55]

A different set of macrocycles, **22**–**24**, were synthesized and investigated by the same group more recently.[11] The tri(ethylene glycol) ester side chains were designed to improve the solubility of the macrocycles in solvents more polar than chloroform, such as acetone, acetonitrile and dimethylsulfoxide (DMSO). In these polar solvents, the hydrocarbon backbones become even more solvophobic. This stronger solvophobic effect was expected to considerably enhance the aromatic interaction and consequently lead to higher aggregate formation. The ethylene glycol ester substituted macrocycle **22** indeed exhibited much larger association constants and aggregates higher than dimer in polar solvents.[11] These results support the conclusion that the solvophobic effect provides a tremendous driving force for aromatic stacking, and therefore, the π–stacking interaction is sensitive to the solvent. Oddly, it was found that macrocycle **22** aggregated even in aromatic solvents such as benzene. The driving force for the stacking under these conditions is currently unknown. Another finding from these studies was that solvophobic forces are incapable of overcoming unfavorable ring electronics. Even in polar environment, very weak association was observed with macrocycles **23** and **24**, having benzyl and phenyl ether linked tri(ethylene glycol) side chains, respectively.

As solvophobic interactions have been demonstrated to favor aromatic stacking, introducing hydrophobic groups into the hydrocarbon skeleton should further intensify the solvophobicity of the backbone in polar solvents and lead to stronger aggregation. To this end, macrocycle **25** with six methyl substituents in the interior of the macrocycle was synthesized and studied. As expected, it exhibited higher aggregation stability than its H-analogue.[61]

More recently, a unique and interesting self-association behavior has been reported for imine-containing macrocycle **4**.[34] Upon replacing a pair of ethynylene units in the backbone with two imino groups, the macrocycle still aggregated in solution, indicating that –C=N– did not severely disrupt π-

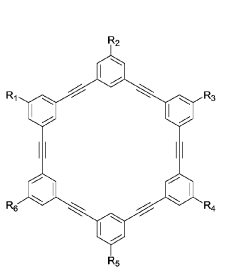

**9**: $R_1 = R_2 = R_3 = R_4 = R_5 = R_6 = CO_2{}^nBu$
**10**: $R_1 = R_2 = R_3 = R_4 = R_5 = R_6 = CO_2{}^nC_7H_{15}$
**11**: $R_1 = R_2 = R_3 = R_4 = R_5 = R_6 = CO_2{}^nC_8H_{17}$
**12**: $R_1 = R_2 = R_3 = R_4 = R_5 = R_6 = CO_2{}^nC_{16}H_{33}$
**13**: $R_1 = R_2 = R_3 = R_4 = R_5 = R_6 = OCO^nBu$
**14**: $R_1 = R_2 = R_3 = R_4 = R_5 = R_6 = O^nBu$
**15**: $R_1 = R_2 = R_3 = R_4 = R_5 = R_6 = CH_2O^nBu$
**16**: $R_1 = R_3 = R_5 = CO_2{}^nBu$, $R_2 = R_4 = R_6 = O^nBu$
**17**: $R_1 = R_2 = R_3 = CO_2{}^nBu$, $R_4 = R_5 = R_6 = O^nBu$
**18**: $R_1 = R_2 = R_3 = R_4 = R_5 = R_6 = CO_2{}^tBu$
**22**: $R_1 = R_2 = R_3 = R_4 = R_5 = R_6 = CO_2(CH_2CH_2O)_3CH_3$
**23**: $R_1 = R_2 = R_3 = R_4 = R_5 = R_6 = CH_2O(CH_2CH_2O)_3CH_3$
**24**: $R_1 = R_2 = R_3 = R_4 = R_5 = R_6 = O(CH_2CH_2O)_3CH_3$
**40**: $R_1 = R_2 = R_3 = CO_2C_6H_{13}$, $R_4 = R_5 = R_6 = OC_6H_{13}$
**43**: $R_1 = R_2 = R_3 = R_4 = CO_2{}^tBu$, $R_5 = R_6 = CO_2^- N^+({}^nC_4H_9)_4$
**44**: $R_1 = R_2 = R_3 = R_4 = R_5 = R_6 = OH$

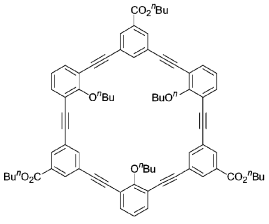

**19**

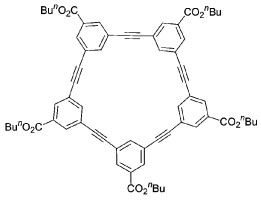

**20**

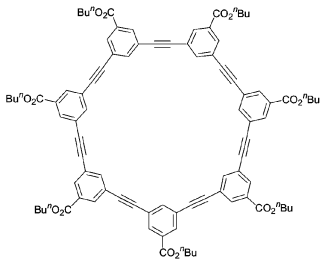

**21**

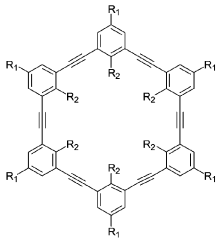

**25**: $R_1 = CO_2(CH_2CH_2O)_3CH_3$, $R_2 = CH_3$
**47**: $R_1 = t\text{-Bu}$, $R_2 = OCH_3$

**Table 1** Self-association data of AEM's.[a]

| compd | Solvent | $K_{assoc.}$ ($M^{-1}$) | $\Delta G$ (kcal $mol^{-1}$) | $\Delta H$ (kcal $mol^{-1}$) | $\Delta S$ (cal $mol^{-1}$ $K^{-1}$) | ref |
|---|---|---|---|---|---|---|
| **9** | $CDCl_3$ | $60^{b,c}$ | $-2.4^b$ | $-5.0 \pm 0.2$ | $-9.2 \pm 0.8$ | 54 |
| **13** | $CDCl_3$ | ~ 0 | | | | 55 |
| **14** | $CDCl_3$ | ~ 0 | | | | 54 |
| **15** | $CDCl_3$ | ~ 0 | | | | 55 |
| **16** | $CDCl_3$ | $18^{b,c}$ | $-1.7^b$ | $-5.6 \pm 0.3$ | $-13.6 \pm 1.0$ | 54 |
| **17** | $CDCl_3$ | $26^{b,c}$ | $-1.9^b$ | $-5.1 \pm 0.3$ | $-10.8 \pm 1.0$ | 54 |
| **18** | $CDCl_3$ | ~ 0 | | | | 55 |
| **19** | $CDCl_3$ | ~ 0 | | | | 55 |
| **20** | $CDCl_3$ | $11^{b,c}$ | $-1.4^b$ | $-3.3 \pm 0.2$ | $-6.6 \pm 0.8$ | 55 |
| **21** | $CDCl_3$ | $16^{b,c}$ | *d* | *d* | *d* | 55 |
| **22** | $CDCl_3$ | $50^{e,f}$ | | | | 11 |
| **22** | THF-$d_8$ | $350^{e,f}$ | | | | 11 |
| **22** | Benzene-$d_6$ | $1200^{e,f}$ | | | | 11 |
| **22** | Acetone-$d_6$ | $15000^{e,f}$ | | | | 11 |
| **24** | Acetone-$d_6$ | $140^{e,f}$ | | | | 11 |
| **28** | $CDCl_3$ | $27.9 \pm 0.7^{c,g}$ | $-2.00 \pm 0.02^g$ | $-5.0 \pm 0.2$ | $-10.0 \pm 0.5$ | 26 |
| **29** | $CDCl_3$ | $28.7 \pm 2.4^{c,g}$ | $-2.02 \pm 0.05^g$ | $-5.7 \pm 0.2$ | $-12.0 \pm 0.7$ | 26 |
| **30** | $CDCl_3$ | $19.9 \pm 1.3^{c,g}$ | $-1.80 \pm 0.04^g$ | $-3.6 \pm 0.2$ | $-6.2 \pm 0.5$ | 26 |
| **31** | $CDCl_3$ | $173 \pm 17^{c,g}$ | $-3.11 \pm 0.07^g$ | $-12.4 \pm 0.5$ | $-30.6 \pm 1.4$ | 26 |
| **32** | $CDCl_3$ | $150 \pm 4^{c,g}$ | $-3.01 \pm 0.02^g$ | $-9.3 \pm 0.5$ | $-21.1 \pm 1.4$ | 26 |
| **33** | $CDCl_3$ | $42.7 \pm 14^{c,g}$ | $-2.26 \pm 0.02^g$ | $-7.4 \pm 0.2$ | $-17.0 \pm 0.7$ | 26 |
| **34** | $CDCl_3$ | $22.8 \pm 0.9^{c,g}$ | $-1.88 \pm 0.02^g$ | $-8.1 \pm 0.2$ | $-20.6 \pm 1.0$ | 26 |
| **30** | Acetone-$d_6$ | $19100 \pm 1900^{f,g}$ | $5.93 \pm 0.07^g$ | | | 26 |
| **30** | $CD_3CN^h$ | $27000^{f,g}$ | $-6.2^g$ | | | 26 |
| **30** | $CD_3OD^h$ | $150000^{f,g}$ | $-7.2^g$ | | | 26 |
| **33** | $CD_3OD^h$ | $580000^{f,g}$ | $-7.9^g$ | | | 26 |
| **28** | Toluene-$d_8{}^h$ | $240^{f,g}$ | $-3.3^g$ | | | 26 |
| **30** | Toluene-$d_8{}^i$ | $163 \pm 11^{f,g}$ | $-3.06 \pm 0.05^g$ | $-6.7 \pm 0.2$ | $-12.2 \pm 0.5$ | 26 |
| **31** | Toluene-$d_8{}^i$ | $210000^{f,g}$ | $-7.4^g$ | $-28.7 \pm 2.4$ | $-71.8 \pm 7.2$ | 26 |
| **33** | Toluene-$d_8{}^i$ | $30000^{f,g}$ | $-6.2^g$ | $-21.5 \pm 0.7$ | $-50.2 \pm 2.4$ | 26 |
| **34** | Toluene-$d_8$ | $340 \pm 70^{f,g}$ | $-3.52 \pm 0.14^g$ | $-28.7 \pm 4.8$ | $-78.9 \pm 12.0$ | 26 |
| **39** | $CD_2Cl_2$/hexane-$d_{14}$ (1:3) | $130 \pm 30^{e,j}$ | | | | 21 |
| **39** | $CD_2Cl_2$/hexane-$d_{14}$ (1:6) | $790 \pm 180^{e,j}$ | | | | 21 |

[a] Determined from NMR chemical shift data; [b] 293 K; [c] based on monomer-dimer model; [d] van't Hoff plot is not linear in the temperature range from 258 to 294 K; [e] room temperature; [f] based on indefinite isodesmic model; [g] 303 K; [h] extrapolated to pure solvent from the plot of $\Delta G$ vs solvent composition; [i] extrapolated from higher temperature data; [j] 298 K.

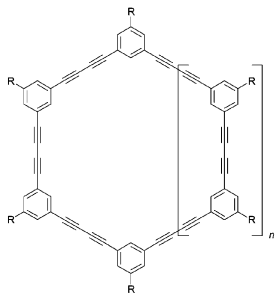

**26**: n = 0, R = $^t$Bu
**27**: n = 2, R = $^t$Bu
**28**: n = 0, R = $CO_2{}^nC_8H_{17}$
**29**: n = 0, R = $CO_2{}^nC_{16}H_{33}$
**30**: n = 0, R = $CO_2(CH_2CH_2O)_3CH_3$
**31**: n = 1, R = $CO_2{}^nC_8H_{17}$
**32**: n = 1, R = $CO_2{}^nC_{16}H_{33}$
**33**: n = 1, R = $CO_2(CH_2CH_2O)_3CH_3$
**34**: n = 2, R = $CO_2{}^nC_8H_{17}$

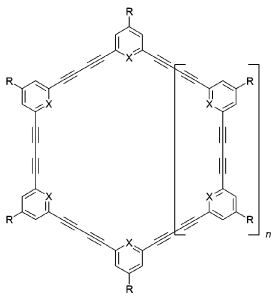

R = $CO_2{}^nC_8H_{17}$
**35**: n = 1, X = C-CN
**36**: n = 1, X = N
**37**: n = 0, X = N

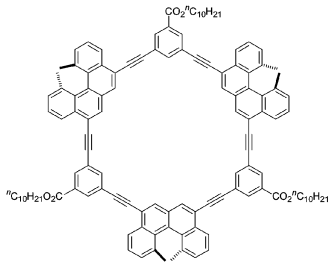

**38**

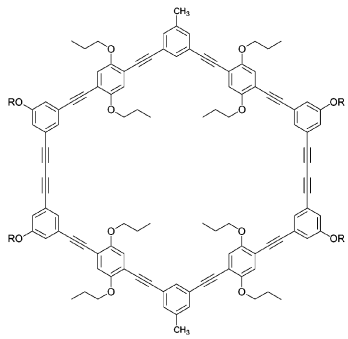

**39**: R = —$CH_2$
**41**: R = $^nC_{18}H_{37}$

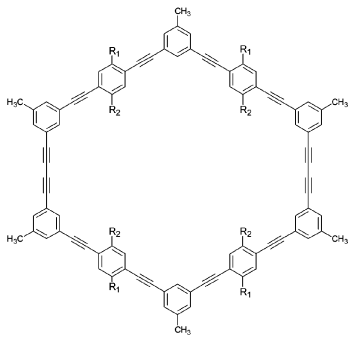

**42**: $R_1 = O^nC_{18}H_{37}$, $R_2 = O^nPr$
**45**: $R_1 = OH$, $R_2 = O^nPr$
**46**: $R_1 = OH$, $R_2 = O^nC_6H_{13}$

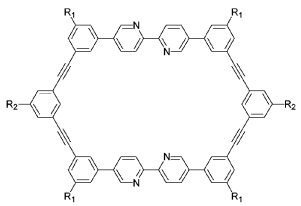

**48**: $R_1 = CH_2OC_6H_{13}$, $R_2 = H$
**49**: $R_1 = CH_2OMOM$, $R_2 = CH_2OC_6H_{13}$
**50**: $R_1 = CH_2OTHP$, $R_2 = CH_2OC_6H_{13}$

stacking interactions. However, the observed concentration dependence of the chemical shift of **4** could not be explained by the isodesmic model unless a tight dimerization is introduced.[56] The extra strength for dimerization was postulated to derive from the dipole-dipole interactions between the imino units of adjacent macrocycles.[34]

Analogous to the *m*-phenylene–ethynylene macrocycles, Tobe et al. investigated self-associations of a series of

macrocycles having *m*-phenylene–diethynylene backbones of different sizes and bearing various side chains.[22,25,26] The envisioned consequences of introducing butadiynylene groups are several fold. First, the macrocycles should demonstrate modified self-association ability due to the different electronic characteristics of the butadiyne group from that of ethynylene unit. Second, an enlarged cyclic cavity resulting from the elongated backbone could avail the binding of large guest molecules.[25,26]

Not surprisingly, macrocycles **26** and **27** did not exhibit concentration dependent chemical shifts since the bulky, electron-donating *tert*-butyl groups disfavor the π–π stacking interaction both sterically and electronically.[25] In contrast, macrocycles **28**–**34**, having linear alkyl or tri(ethylene glycol) ester side chains, exhibited strong upfield shifting at increased concentration in a series of different solvents or solvent mixtures, indicating the occurrence of π-stacked aggregates.[26] Assuming that monomer–dimer equilibrium was the predominant association process in chloroform and that higher aggregates formed in polar solvents, the association constants of these macrocycles in a series of solvents were obtained (directly or through extrapolation), by fitting the experimental NMR and VPO data to the models describing the corresponding association behaviors. The association constants were then compared to those of *m*-phenylene–ethynylene macrocycles containing the same number of phenylene units and the same type of side chain structures in the corresponding solvent (Table 1). These studies further confirmed previous conclusions about aromatic stacking of the *m*-phenylene–ethynylene macrocycles, *e.g.*, solvophobic interactions and electron-withdrawing substituents strongly favor self-association while the side chain length has little influence in the process. More importantly, a series of distinct behaviors were disclosed by these phenylene–diethynylene macrocycles. Higher self-association constants than those of the corresponding *m*-phenylene–ethynylene macrocycles were observed, and they were attributed to the stronger electron-withdrawing ability of the butadiyne groups. This proposition was supported by the calculated electrostatic potential profiles of the model compounds, showing that the phenylene–diethynylene backbone is more electron-deficient than the analogous phenylene–ethynylene framework. Consistently, thermodynamic parameters determined based on variable temperature NMR study indicated that the extra driving force favoring the association comes from a larger enthalpy change.[26]

Although the qualitative association propensities were consistent, discrepancy occurred between the calculated association constants based on NMR and VPO measurements. VPO tended to afford higher association constants than NMR when dimerization predominated; while smaller values were observed by VPO when higher order association became significant. Such discrepancies may have resulted from the sensitivities of the two techniques to different sized aggregates.

Analogous phenylene–diethynylene macrocycles **35**–**37**, with spatially defined *endo*-annular cyano- or pyridino- functionalities were also synthesized by Tobe *et al.*[23,24] They were envisioned to bind guest molecules into the cavity through non-covalent ion–dipole or hydrogen-bonding interactions. Although these macrocycles did not self-associate in chloroform, they each formed hetero-aggregates with macrocycle **31**, giving rise to association constants even higher than that of the homodimer of **31**. The absence of the self-association in **35** and **36** was attributed to intermolecular electrostatic repulsion among the cyano- or pyridino- groups. Additionally, molecular simulations suggested that this repulsion may have forced macrocycle **35** to adopt a nonplanar conformation, which could further preclude the self-association.[23] The heteroaggregation between **31** and **35**, or **36**, was postulated to be driven by dipolar interactions between the phenylene and the electron-deficient cyanophenylene/pyridine units. The tetrameric pyridine–diethynylene macrocycle **37** exhibited similar association behavior with **36** in solution, while its analogue, tetrakis(4-cyanophenylene–diethynylene) macrocycle, was reported to be synthetically not accessible, presumably due to the ring strain related to the electrostatic and steric repulsions.[24] The heteroaggregation process was shown to be sensitive to ring-size matching; that is, macrocycles with complementary electrostatic properties but mismatched ring size (*e.g.*, **28** and **36** or **31** and **37**) did not form heteroaggregates.[24]

The self-association of a set of macrocycles containing novel, chiral helicene units in the backbone (**38**) was investigated by Yamaguchi and coworkers.[38] VPO and NMR studies demonstrated that only dimers formed in chloroform and benzene. Interestingly, the chirality of the helicenes strongly influenced the aggregate stability. The dimerization of (*M*,*M*,*M*)-**38** was the most stable, and the stability of the homodimer of its diastereomer (*M*,*P*,*M*)-**38** was significantly diminished. While aggregation among components of a racemic mixture of (*M*,*M*,*M*)- and (*P*,*P*,*P*)-**38** was weaker than both homodimers, it was still stronger than that of the (*M*,*P*,*M*)- and (*P*,*M*,*P*)-**38** mixture.

Höger and coworkers have exploited the special properties of a distinct group of AEMs in their supramolecular studies. In a variety of chlorinated and aromatic solvents, macrocycle **39** exhibit good solubility but no aggregation. However, concentration dependent chemical shifts were observed upon adding the apolar solvent hexane into $CD_2Cl_2$ solution. The dimerization constant increased with increasing hexane composition in the binary solvent mixture, indicating the solvophobic nature of the association (Table 1).[21] Combining the results from these and the independent studies on polar solvents induced aromatic associations carried out by different groups, it can be concluded that aromatic stacking can take place in both polar and apolar solvents. The aromatic backbone of AEMs is best solvated by chlorohydrocarbon solvents such as chloroform and methylene chloride, possibly due to C–H···π interactions. Under either more (*e.g.*, in acetonitrile) or less polar (*e.g.*, in hexane) environments, solvophobic association occurs and contributes to aromatic stacking. Therefore, π–π stacking can be induced by either increasing or decreasing the solvent polarity. Accordingly, provided appropriate side chains are present to maintain solubility, aggregates of AEMs can form under either solvent polarity extreme, driven by the aromatic and solvophobic interactions.[62]

A novel coil–ring–coil structure was developed in Höger's laboratory by joining a pair of narrowly dispersed polystyrene oligomers with an AEM.[46,63] These coil–ring–coil polymers were soluble in cylcohexane at an elevated temperature and the resulting solutions were found to be birefringent, suggesting formation of ordered structures. Dynamic light scattering studies in cyclohexane disclosed a coexistence of discrete, monomeric coil–ring–coil molecules together with some much larger species. X-ray scattering revealed that these larger entities were of a hollow cylindrical shape, with an inner diameter consistent with that of the macrocycle's cavity and an average length of about 500 nm. TEM and AFM images further confirmed the existence of such long, cylindrical aggregates.[46]

## Associations in bulk phases

**Liquid crystalline mesophases**. Ever since the discotic liquid crystal (LC) was first reported more than two decades ago,[64] this area has attracted considerable interest. AEMs have been intensely studied as candidates for mesogens of columnar LCs, due to their non-collapsible disk-shaped frameworks. The

tubular LC mesophase of AEM **40** was first observed and characterized using optical microscopy, DSC and powder X-ray diffraction.[65,66]

More recently, Höger *et al.* discovered a different AEM having the discotic LC phase, and a particularly unique and interesting architectural motif was elucidated. Surprisingly at first sight, only one of the two macrocycles, **41** and **42**, with very similar structures exhibited a thermotropic LC mesophase.[67] A subsequently obtained single crystal structure revealed that, the aliphatic side chains of macrocycle **42**, the one that has the mesophase, were pointing inside the macrocycle in the solid state, filling the internal cavity void. This observation, together with the absence of the LC phase in the other macrocycle, **41**, led these researchers to speculate that the free rotation of the *para*-phenylene[17,68,69] was responsible for the occurrence of the LC phase. This rotational freedom allowed the long side chains of **42** to fold back into the cavity of their own backbone. The adaptable orientation of the side chain was proposed to have eliminated intermolecular entanglements and side chain–cavity interpenetration and hence entailed the molecular mobility required for the occurrence of the mesophase.[67] Such an arrangement would obviously not be possible for **41** in which the side chains are attached to the periphery of the corner pieces of the backbone.

**Self-assembly at the air/water interface**. The rigid discotic shape of AEMs and their intrinsic tendency to self-assemble into columnar aggregates have made them suitable building blocks for fabricating highly ordered monolayer films. The cavity of the macrocycles can spontaneously align and form long tubular channels within the monolayer. Such a unique structure may endow the film with novel properties that have potentials for molecular based separations.

A highly ordered monolayer at the air/water interface has been reported to form by some amphiphilic AEMs.[70,71] It was found that the orientation of these macrocycles at the air/water interface was sensitive to the structure and the spatial arrangement of the peripheral functional groups. Macrocycles with spatially segregated alkyl and carboxylate side groups (*e.g.*, **43**) formed ordered, compact monolayers by adopting an edge-on orientation, generating tubular channels parallel to the interface.[70] However, only poorly ordered and less stable monolayers were obtained from macrocycles having exclusively hydrophilic side groups; and the calculated average molecular area of these monolayers did not agree with a face-on orientation of the macrocycle. Additionally, it was demonstrated that the edge-on monolayers could be further stabilized by the addition of KCl salt in the aqueous subphase, presumably by strengthening the intermolecular, intracolumnar interactions.[71]

**Solid state structures**. The available single crystal structures of AEMs have demonstrated a variety of highly ordered packing motifs in the solid state, commonly featured with uniform micro-porosity or tubular channels. A two dimensional hexagonal network, studied by Venkataraman *et al.*, was illustrated by macrocycle **44**.[72] Stabilized through intermolecular H-bonds between the phenolic groups on the adjacent macrocycles, the hexagonal motif naturally followed from the geometric shape of the modular units. The two-dimensional layered structures stacked in an …ABCABC… sequence of cubic closest packing in the third dimension. Extended channels thus arose from aligned, alternate macrocycle cavities and voids defined by H-bonded circuits between the adjacent macrocycles (Fig. 5).

Recently, a very interesting observation was reported by Höger *et al.*: solvent triggers the conformational transition of an AEM.[73] In the single crystal structure of an amphiphilic AEM, **45**, the molecule existed in a planar conformation. A large

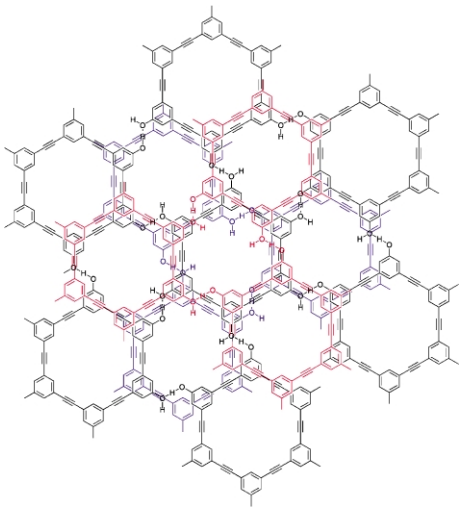

**Fig. 5** Schematic packing of three layers of H-bonded **44** in an …ABCABC…layered sequence of cubic closest packing (peripheral–OH groups are omitted for clarity; blue–lower layer, black–middle layer, red–top layer).[72]

number of solvent molecules (pyridine) coordinated to the phenolic units from the macrocycle exterior, leaving the hydrophobic propyl group filling the inside of the cavity.[17] Based on this observation, it was envisioned that, due to the free rotation about the *para*-phenylene moieties,[17,69] the conformation of such an amphiphilic macrocycle should be adaptable to the polarity of the solvent, resulting in either a hydrophilic or a hydrophobic cavity. This suggestion has been proven correct in a more recent report.[73] It was demonstrated that macrocycle **46** could exist in two different conformational states dictated by the solvent. The single crystal structure of **46** obtained from pyridine solution revealed a conformational state with the cavity filled with two *n*-hexyloxy chains and two hydroxy groups H-bonded to solvent molecules, while the other two *n*-hexyloxy and hydroxy units (also H-bonded to pyridines) resided on the outside of the ring. In contrast, for crystals grown in a less polar solvent (THF), all of the hydroxy units were found on the inside of the cavity, together with 12 THF molecules, four of which formed H-bonds with the hydroxy groups of the macrocycle. In both cases, the macrocycle stacked face-to-face, forming extended tubular channels with aligned void cavities.

In the crystal structure of Bunz's AEM **3**, all the macrocycles were also aligned and stacking into columns. However, the plane of the macrocycle was significantly tilted with respect to the columnar axis, and the macrocycles in one column were not parallel to those in the neighboring columns. Such a packing motif may be a result of minimizing the steric repulsion among the bulky *tert*-butyl substituents.[31]

In contrast, when this *tert*-butyl substituted macrocycle was decorated with six methoxy groups on the interior (*i.e.*, **47**), common features of AEMs solid-state structure, such as planar ring conformation, two-dimensional hexagonal packing with an …ABCABC… layered sequence in the third dimension, and tubular channels, were all preserved. Moreover, the single crystal structure of this compound also showed that the *endo*-annular methyl groups were pointed alternatively up and down, reaching out of the plane of the cyclic framework, most likely driven by the intra-ring, steric repulsions or the intermolecular, van der Waals interactions.[74]

Schlüter and coworkers demonstrated that macrocycles having a bipyridino-functionalized backbone could also form layered structures having channels. These macrocycles maintained an overall planar conformation in the solid state with the bipyridine units slightly tilted out of the plane.[36,37] Interestingly, three macrocycles, **48**–**50**, having the same backbone

but slightly different side chain structures exhibited three different solid-state packing motifs. Although all of them contained a similarly layered structure and extended channels, the observation of variation suggested that the solid-state structure of AEMs is very sensitive to subtle changes in the side chains.

More recently, Tykwinski and coworkers reported a novel solid-state structure exhibited by an AEM: macrocycles bound in pair, face-to-face, joined by the Pt metal ions coordinated to the pyridine units incorporated at the opposite end of the macrocycle backbone. This unique packing motif endows the bulk material with novel bidirectional porosity.[75]

## Conclusions and perspectives

Significant developments have taken place within the last two decades in the syntheses and supramolecular chemistry of AEMs. A set of versatile and efficient synthetic methodologies have provided the potential for producing AEMs to meet diverse design requirements. With a much better understanding of the noncovalent interactions, chemists have acquired more powerful tools for rationally designing and constructing highly complex but well-defined supramolecular assemblies. With the convenient syntheses and the extraordinary self-assembling capability, AEMs have presented themselves as promising modular building blocks for a variety of structures, such as ion channels, liquid crystalline materials, molecular electronic or optical devices, microscopic reactors, microporous solids, *etc*. Moreover, the unique geometric shape of AEMs has made them attractive candidates as host molecules.[23,24,69,74] Size, polarity and functional group complementary between the host and the guest molecules is obviously a critical factor in host–guest design, and AEMs can be conveniently tailored in response to the variation of the guest molecules. Host–guest chemistry may represent another promising future direction in which the AEMs will be developed.

## Acknowledgements

Work in the authors' laboratory was supported by the National Science Foundation and the U.S. Department of Energy, Division of Material Science, through the Frederick Seitz Materials Research Laboratory at the University of Illinois at Urbana-Champaign.

## Notes and references

1 J. S. Moore, *Acc. Chem. Res.*, 1997, **30**, 402.
2 R. Faust, *Angew. Chem., Int. Ed.*, 1998, **37**, 2825.
3 U. H. F. Bunz, Y. Rubin and Y. Tobe, *Chem. Soc. Rev.*, 1999, **28**, 107.
4 S. Höger, *J. Polym. Sci. Part A: Polym. Chem.*, 1999, **37**, 2685.
5 M. M. Haley, J. J. Pak and S. C. Brand, *Top. Curr. Chem.*, 1999, **201**, 81.
6 J. K. Young and J. S. Moore, 'Acetylene in nanostructures', in *Modern Aectylene Chemistry*, ed. P. J. Stang and F. Diederich, VCH, Weinheim, 1995, ch. 12.
7 K. Sonogashira, *Comprehensive Organic Synthesis*, ed. B. M. Trost and I. Fleming, Pergamon Press, Oxford, 1991, vol. 3, p. 521.
8 K. Sonogashira, Y. Tohda and N. Hagihara, *Tetrahedron Lett.*, 1975, 4467; L. Cassar, *J. Organomet. Chem.*, 1975, **93**, 253; H. A. Dieck and R. F. Heck, *J. Organomet. Chem.*, 1975, **93**, 259.
9 J. S. Moore and J. Zhang, *Angew. Chem., Int. Ed. Engl.*, 1992, **31**, 922.
10 J. Zhang, D. J. Pesak, J. L. Ludwick and J. S. Moore, *J. Am. Chem. Soc.*, 1994, **116**, 4227.
11 S. Lahiri, J. L. Thompson and J. S. Moore, *J. Am. Chem. Soc.*, 2000, **122**, 11315.
12 U. H. F. Bunz, *Chem. Rev.*, 2000, **100**, 1605.
13 A. S. Hay, *J. Org. Chem.*, 1962, **27**, 3320.
14 G. Eglinton and A. R. Galbraith, *J. Chem. Soc.*, 1959, 889; O. M. Behr, G. Eglinton, A. R. Galbraith and R. A. Raphael, *J. Chem. Soc.*, 1960, 3614; D. O'Krongly, S. R. Denmeade, M. Y. Chiang and R. Breslow, *J. Am. Chem. Soc.*, 1985, **107**, 5544.
15 C. Cai and A. Vasella, *Helv. Chim. Acta*, 1995, **78**, 2053.
16 For a review on acetylene coupling: P. Siemsen, R. C. Livingston and F. Diederich, *Angew. Chem., Int. Ed.*, 2000, **39**, 2632.
17 S. Höger and V. Enkelmann, *Angew. Chem., Int. Ed. Engl.*, 1995, **34**, 2713.
18 S. Höger, A. D. Meckenstock and H. Pellen, *J. Org. Chem.*, 1997, **62**, 4556.
19 S. Höger, A. D. Meckenstock and S. Müller, *Chem. Eur. J.*, 1998, **4**, 2423.
20 S. Höger and A. D. Meckenstock, *Chem. Eur. J.*, 1999, **5**, 1686.
21 S. Höger, K. Bonrad, A. Mourran, U. Beginn and M. Möller, *J. Am. Chem. Soc.*, 2001, **123**, 5651.
22 Y. Tobe, N. Utsumi, K. Kawabata and K. Naemura, *Tetrahedron Lett.*, 1996, **37**, 9325.
23 Y. Tobe, N. Utsumi, A. Nagano and K. Naemura, *Angew. Chem., Int. Ed.*, 1998, **37**, 1285.
24 Y. Tobe, A. Nagano, K. Kawabata, M. Sonoda and K. Naemura, *Org. Lett.*, 2000, **2**, 3265.
25 Y. Tobe, N. Utsumi, A. Nagano, M. Sonoda and K. Naemura, *Tetrahedron*, 2001, **57**, 8075.
26 Y. Tobe, N. Utsumi, K. Kawabata, A. Nagano, K. Adachi, S. Araki, M. Sonoda, K. Hirose and K. Naemura, *J. Am. Chem. Soc.*, 2002, **124**, 5350.
27 V. Hensel, K. Lützow, J. Jacob, K. Gessler, W. Saenger and A. D. Schlüter, *Angew. Chem., Int. Ed. Engl.*, 1997, **36**, 2654.
28 V. Hensel and A. D. Schlüter, *Chem. Eur. J.*, 1999, **5**, 421.
29 U. Lehmann and A. D. Schlüter, *Eur. J. Org. Chem.*, 2000, 3483.
30 H. A. Staab and K. Neunhoeffer, *Synthesis*, 1974, 424.
31 P.-H. Ge, W. Fu, W. A. Herrmann, E. Herdtweck, C. Campana, R. D. Adams and U. H. F. Bunz, *Angew. Chem., Int. Ed.*, 2000, **39**, 3607.
32 S. A. Krouse and R. R. Schrock, *Macromolecules*, 1989, **22**, 2569; X. P. Zhang and G. C. Bazan, *Macromolecules*, 1994, **27**, 4627; U. H. F. Bunz and L. Kloppenburg, *Angew. Chem., Int. Ed.*, 1999, **38**, 478.
33 U. H. F. Bunz, *Acc. Chem. Res.*, 2001, **34**, 998.
34 D. Zhao and J. S. Moore, *J. Org. Chem.*, 2002, **67**, 3548.
35 Z. Wu and J. S. Moore, *Angew. Chem., Int. Ed. Engl.*, 1996, **35**, 297.
36 O. Henze, D. Lentz and A. D. Schlüter, *Chem. Eur. J.*, 2000, **6**, 2362.
37 O. Henze, D. Lentz, A. Schäfer, P. Franke and A. D. Schlüter, *Chem. Eur. J.*, 2002, **8**, 357.
38 K. Nakamura, H. Okubo and M. Yamaguchi, *Org. Lett.*, 2001, **3**, 1097.
39 D. Zhao and J. S. Moore, unpublished results.
40 J. K. Young, J. C. Nelson and J. S. Moore, *J. Am. Chem. Soc.*, 1994, **116**, 10841; J. C. Nelson, J. K. Young and J. S. Moore, *J. Org. Chem.*, 1996, **61**, 8160.
41 M. Rothe, M. Lohmüller, U. Breuksch and G. Schmidtberg, *Angew. Chem., Int. Ed. Engl.*, 1994, **33**, 1960.
42 D. B. Shortell, L. C. Palmer and J. M. Tour, *Tetrahedron*, 2001, **57**, 9055.
43 H. L. Anderson and J. K. M. Sanders, *Angew. Chem., Int. Ed. Engl.*, 1990, **29**, 1400; D. W. J. McCallien and J. K. M. Sanders, *J. Am. Chem. Soc.*, 1995, **117**, 6611.
44 S. J. Rowan, S. J. Cantrill, G. R. L. Cousins, J. K. M. Sanders and J. F. Stoddart, *Angew. Chem., Int. Ed.*, 2002, **41**, 898.
45 D. J. Hill and J. S. Moore, *Proc. Natl. Acad. Sci. USA*, 2002, **99**, 5053.
46 S. Rosselli, A. D. Ramminger, T. Wagner, B. Silier, S. Wiegand, W. Häußler, G. Lieser, V. Scheumann and S. Höger, *Angew. Chem., Int. Ed.*, 2001, **40**, 3137.
47 For a recent review on aromatic interactions: C. A. Hunter, K. R. Lawson, J. Perkins and C. J. Urch, *J. Chem. Soc., Perkin Trans. 2*, 2001, 651.
48 C. A. Hunter and J. K. M. Sanders, *J. Am. Chem. Soc.*, 1990, **112**, 5525.
49 M. S. Cubberly and B. L. Iverson, *J. Am. Chem. Soc.*, 2001, **123**, 7560.
50 R. L. Jaffe and G. D. Smith, *J. Chem. Phys.*, 1996, **105**, 2780.
51 D. B. Smithrud and F. Diederich, *J. Am. Chem. Soc.*, 1990, **112**, 339.
52 A. V. Muehldorf, D. Van Engen, J. C. Warner and A. D. Hamilton, *J. Am. Chem. Soc.*, 1988, **110**, 6561.
53 S. C. Zimmerman, K. W. Saionz and Z. J. Zeng, *Proc. Natl. Acad. Sci.*, 1993, **90**, 1190; S. C. Zimmerman and K. W. Saionz, *J. Am. Chem. Soc.*, 1995, **117**, 1175.
54 J. Zhang and J. S. Moore, *J. Am. Chem. Soc.*, 1992, **114**, 9701.
55 A. S. Shetty, J. Zhang and J. S. Moore, *J. Am. Chem. Soc.*, 1996, **118**, 1019.

56 R. B. Martin, *Chem. Rev.*, 1996, **96**, 3043.
57 C. Giessner-Prettre, B. Pullman, P. N. Borer, L.-S. Kan and P. O. P. Ts'O, *Biopolymers*, 1976, **15**, 2277.
58 M. Sauders and J. B. Hyne, *J. Chem. Phys.*, 1958, **29**, 1319; S. H. Marcus and S. I. Miller, *J. Am. Chem. Soc.*, 1966, **88**, 3719; I. Horman and B. Dreux, *Helv. Chim. Acta*, 1984, **67**, 754.
59 P. O. Ts'o and S. I. Chan, *J. Am. Chem. Soc.*, 1964, **86**, 4176.
60 F. J. C. Rossotti and H. Rossotti, *J. Phys. Chem.*, 1961, **65**, 930.
61 R. B. Prince, Ph.D. Thesis, University of Illinois, 2000.
62 Analogous observations of solvophobically driven intramolecular aromatic stacking of *m*-phenylene–ethynylene oligomers in apolar solvent: L. Brunsveld, R. B. Prince, E. W. Meijer and J. S. Moore, *Org. Lett.*, 2000, **2**, 1525.
63 S. Höger, K. Bonrad, S. Rosselle, A. D. Ramminger, T. Wagner, B. Silier, S. Wiegand, W. Häußler, G. Lieser and V. Scheumann, *Macromol. Symp.*, 2002, **177**, 185.
64 S. Chandrasekhar, B. K. Sadashiva and K. A. Suresh, *Pramana*, 1977, **9**, 471.
65 J. Zhang and J. S. Moore, *J. Am. Chem. Soc.*, 1994, **116**, 2655.
66 O. Y. Mindyuk, M. R. Stetzer, P. A. Heiney, J. C. Nelson and J. S. Moore, *Adv. Mater.*, 1998, **10**, 1363.
67 S. Höger, V. Enkelmann, K. Borad and C. Tschierske, *Angew. Chem., Int. Ed.*, 2000, **39**, 2267.
68 T. C. Bedard and J. S. Moore, *J. Am. Chem. Soc.*, 1995, **117**, 10662.
69 D. L. Morrison and S. Höger, *Chem. Commun.*, 1996, 2313.
70 A. S. Shetty, P. R. Fischer, K. F. Stork, P. W. Bohn and J. S. Moore, *J. Am. Chem. Soc.*, 1996, **118**, 9409.
71 O. Y. Mindyuk, M. R. Stetzer, D. Gidalefitz, O. A. Heiney, J. C. Nelson and J. S. Moore, *Langmuir*, 1999, **15**, 6897.
72 D. Venkataraman, S. Lee, J. Zhang and J. S. Moore, *Nature*, 1994, **371**, 591.
73 S. Höger, D. L. Morrison and V. Enkelmann, *J. Am. Chem. Soc.*, 2002, **124**, 6734.
74 Y. Hosokawa, T. Kawase and M. Oda, *Chem. Commun.*, 2001, 1948.
75 K. Campbell, C. J. Kuehl, M. J. Ferguson, P. J. Stang and R. R. Tykwinski, *J. Am. Chem. Soc.*, 2002, **124**, 7266.